Acta Cryst E CRYSTALLOGRAPHIC COMMUNICATIONS

ISSN 2056-9890

Coupling between 2-pyridylselenyl chloride and phenylselenocyanate: synthesis, crystal structure and non-covalent interactions

Ayalew W. Temesgen,[a] Alexander G. Tskhovrebov,[b] Alexey A. Artemjev,[b] Alexey S. Kubasov,[c] Alexander S. Novikov,[d] Alexander V. Borisov,[e] Anatoly A. Kirichuk,[b] Andreii S. Kritchenkov[b] and Tuan Anh Le[f]*

[a]Department of Chemistry, College of Natural and Computational Science, University of Gondar, Gondar 196, Ethiopia, [b]People's Friendship University of Russia, 6 Miklukho-Maklaya Street, Moscow, 117198, Russian Federation, [c]Kurnakov Institute of General and Inorganic Chemistry, Russian Academy of Sciences, Leninsky Prosp. 31, 119071, Moscow, Russian Federation, [d]Institute of Chemistry, Saint Petersburg State University, Universitetskaya, Nab., 7/9, 199034 Saint Petersburg, Russian Federation, [e]R.E. Alekseev Nizhny Novgorod State Technical University, Minin St., 24, Nizhny, Novgorod, Russian Federation, and [f]University of Science, Vietnam National University, Hanoi, 334 Nguyen Trai, Thanh Xuan, Hanoi, 100000, Vietnam. *Correspondence e-mail: wodajo.ayalew@uog.edu.et

Received 14 November 2023
Accepted 10 September 2024

Edited by J. M. Delgado, Universidad de Los Andes, Venezuela

This article is part of a collection of articles to commemorate the founding of the African Crystallographic Association and the 75th anniversary of the IUCr.

Keywords: crystal structure; non-covalent interactions; chalcogen heterocycles; chalcogen bonding.

CCDC reference: 2382988

Supporting information: this article has supporting information at journals.iucr.org/e

A new pyridine-fused selenodiazolium salt, 3-(phenylselanyl)[1,2,4]selenadiazolo[4,5-*a*]pyridin-4-ylium chloride dichloromethane 0.352-solvate, $C_{12}H_9N_2Se_2^+\cdot Cl^-\cdot 0.352CH_2Cl_2$, was obtained from the reaction between 2-pyridylselenenyl chloride and phenylselenocyanate. Single-crystal structural analysis revealed the presence of C—H···N, C—H···Cl^-, C—H···Se hydrogen bonds as well as chalcogen–chalcogen (Se···Se) and chalcogen–halogen (Se···Cl^-) interactions. Non-covalent interactions were explored by DFT calculations followed by topological analysis of the electron density distribution (QTAIM analysis). The structure consists of pairs of selenodiazolium moieties arranged in a head-to-tail fashion surrounding disordered dichloromethane molecules. The assemblies are connected by C—H···Cl^- and C—H···N hydrogen bonds, forming layers, which stack along the *c*-axis direction connected by bifurcated Se···Cl^-···H—C interactions.

1. Chemical context

Recently, a novel cycloaddition reaction between nitriles and 2-pyridylselenyl reagents was described (Khrustalev *et al.*, 2021). What makes this finding particularly notable is that the reaction takes place under mild conditions, displaying a high degree of chemoselectivity (Grudova *et al.*, 2022; Artemjev *et al.*, 2023). As a result, pyridinium-fused selenodiazolium salts are formed with excellent yields.

As part of our ongoing project to investigate the reactivity of bifunctional 2-pyridylselenyl reagents (Grudova *et al.*, 2022; Artemjev *et al.*, 2022, 2023; Sapronov *et al.*, 2023) we have recently expanded our research to explore the chemistry of addition to the C≡N triple bond involving a different category of nitrile substrates known as cyanamides or push–pull nitriles. Push–pull structures are characterized by high polarization and consist of an electron-withdrawing substituent or electronegative atom on one side of the multiple bond and an electron-donating group on the opposite side (Le Questel *et al.*, 2000; Gushchin *et al.*, 2009; Kritchenkov *et al.*, 2011).

Here we show that 2-pyridylselenyl chloride reacts efficiently with phenylselenocyanate furnishing a cationic pyridinium-fused 1,2,4-selenodiazole in high yield. This finding is another illustration of the remarkable propensity of bifunctional 2-pyridylselenyl reagents to engage in dipolar cyclo-

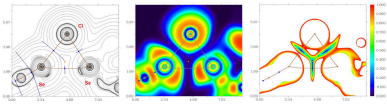

OPEN ACCESS
Published under a CC BY 4.0 licence

addition with the CN triple bond, displaying a high degree of chemoselectivity. The title compound was synthesized in high yield in CH_2Cl_2 according to the scheme.

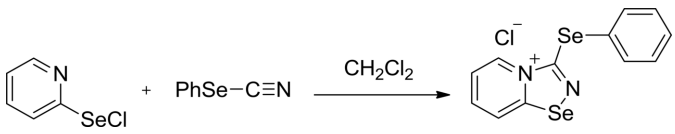

2. Structural commentary

Crystals suitable for X-ray analysis were obtained directly from the reaction mixture. The compound crystallized as colorless blocks in space group $P2_1/c$. The asymmetric unit (Fig. 1) contains one cation, one Cl^- anion and a disordered CH_2Cl_2 molecule. The 1,2,4-selenodiazole fragment is almost planar (r.m.s.d. = 0.017 Å) and makes an angle of 81.64 (16)° with the phenylselenyl ring. The Se1—N2 and Se1—C1 bond lengths are 1.863 (4) and 1.877 (4) Å, respectively, and the Se1···Cl1 distance is 2.9325 (17). These bond distances are similar to those reported in previous work on 1,2,4-selenodiazoles (Grudova *et al.*, 2022; Artemjev *et al.*, 2022, 2023; Sapronov *et al.*, 2022, 2023). The Se2—C6 and Se2—C7 bond lengths are typical for Se—C_{ar} bonds [1.926 (5) Å and 1.946 (5) Å, respectively]. The C7—Se2—C6—N1 and C6—Se2—C7—C12 torsion angles are 93.4 (5) and 76.9 (4)°, respectively.

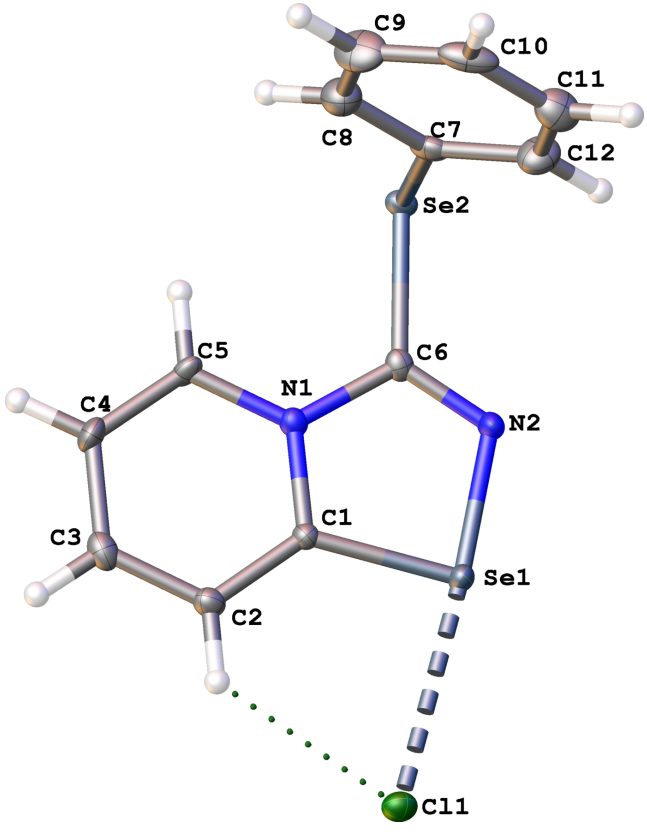

Figure 1
Molecular structure of the title compound. Displacement ellipsoids are drawn at the 50% probability level.

Table 1
Hydrogen-bond geometry (Å, °).

D—H···A	D—H	H···A	D···A	D—H···A
C2—H2···Cl1	0.95	2.60	3.297 (5)	131
C3—H3···Cl1^{i}	0.95	2.60	3.526 (5)	167
C5—H5···Se2	0.95	2.82	3.242 (5)	108
C5—H5···N2^{ii}	0.95	2.45	3.179 (6)	134

Symmetry codes: (i) $x, -y+\frac{1}{2}, z+\frac{1}{2}$; (ii) $x, -y+\frac{3}{2}, z+\frac{1}{2}$.

3. Supramolecular features

The crystal packing is shown in Fig. 2, viewed down the *b* axis. In the crystal, pairs of selenodiazolium moieties are arranged in a head-to-tail fashion surrounding disordered dichloromethane molecules. C—H···Cl^- and C—H···N hydrogen bonds (Table 1) connect these units to form layers parallel to the *ac* plane. In addition, π–π stacking interactions between the phenyl rings of two neighboring molecules occur. The layers are interconnected via bifurcated Se···Cl^-···H—C interactions and stack along the *c*-axis.

To further understand the nature of the interactions and to quantify the strength of the bifurcated chalcogen–halogen–hydrogen contacts, Se···Cl^-···H—C, and the interactions involving the Se atom (Se···Se and Se···Cl^-) in the crystal structure, DFT calculations followed by a topological analysis of the electron-density distribution (QTAIM analysis) were carried out at the ωB97XD/6-311++G** level of theory for the model structure (see Computational details and Table S1 in the supporting information). The results of the QTAIM analysis are summarized in Table S1. The contour line diagrams of the Laplacian of the electron density distribution $\tilde{N}^2r(\mathbf{r})$, bond paths, and selected zero-flux surfaces, visualization of electron localization function (ELF) and reduced density gradient (RDG) analyses for bifurcated

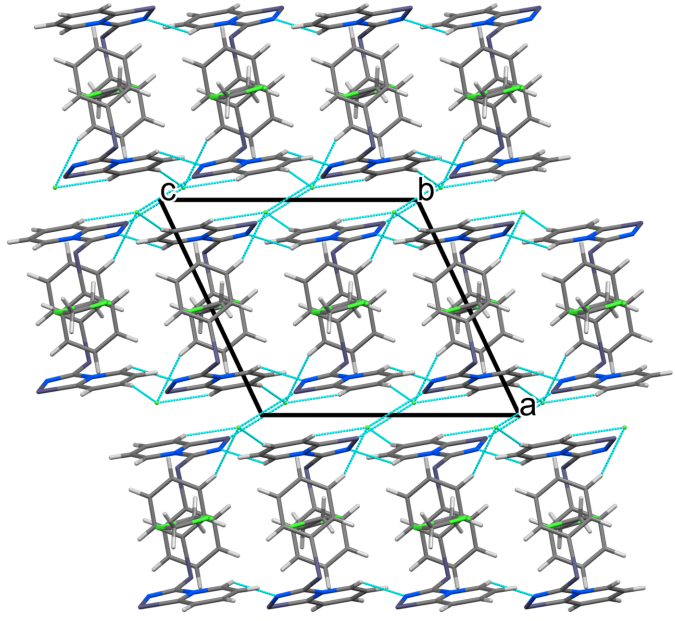

Figure 2
View along the *b* axis of the crystal packing of the title compound.

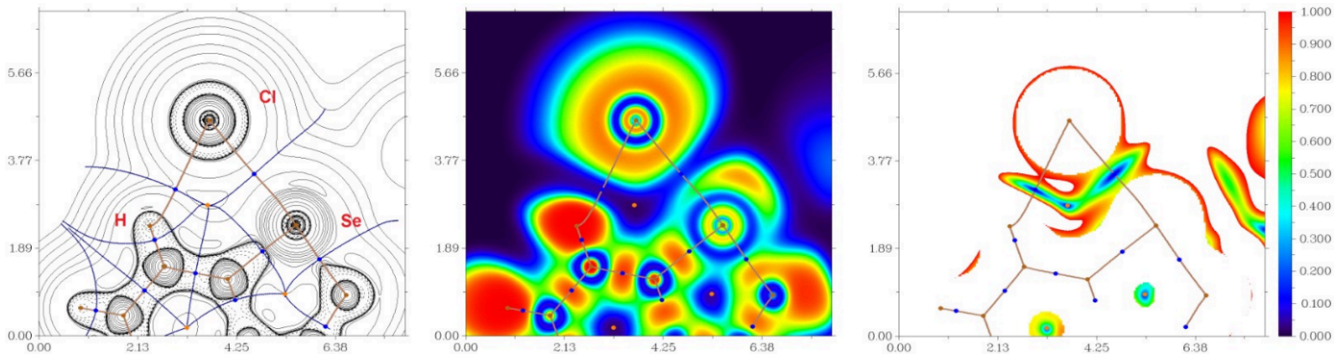

Figure 3
Contour line diagram of the Laplacian of the electron-density distribution $\tilde{N}^2 r(\mathbf{r})$, bond paths, and selected zero-flux surfaces (left panel), visualization of the electron localization function (ELF, center panel) and reduced density gradient (RDG, right panel) analyses for bifurcated chalcogen-hydrogen bonding Se···Cl$^-$···H—C (contacts Se1···Cl1$^-$ 2.9325 (17) Å and C2—H2···Cl$^-$ 2.60 Å) in the crystal structure. Bond critical points (3, −1) are shown in blue, nuclear critical points (3, −3) in pale brown, ring critical points (3, +1) in orange, bond paths are shown as pale brown lines, length units in Å, and the color scale for the ELF and RDG maps is presented in a.u.

Se···Cl$^-$···H—C, Se···Se and Se···Cl$^-$ interactions in the crystal structure are shown in Figs. 3 and 4, respectively.

The QTAIM analysis of the model structure demonstrates the presence of bond critical points (3, −1) for short contacts Se···Cl$^-$, C–H···Cl$^-$ and Se···Se in the crystal structure (Table S1 and Figs. 3 and 4) (Bondi *et al.*, 1966). The low magnitude of the electron density, the positive values of the Laplacian of the electron density and zero or very close to zero values of the energy density in these bond critical points (3, −1) and estimated strength for appropriate short contacts are typical for weak purely non-covalent [$-G(\mathbf{r})/V(\mathbf{r}) > 1$; Espinosa *et al.*, 2002] interactions. The Laplacian of the electron density is typically decomposed into the sum of contributions along the three principal axes of maximal variation. The three eigenvalues of the Hessian matrix (λ_1, λ_2 and λ_3) and the sign of λ_2 can be utilized to distinguish bonding (attractive, $\lambda_2 < 0$) weak interactions from non-bonding ones (repulsive, $\lambda_2 > 0$) (Johnson *et al.*, 2010; Contreras-García *et al.*, 2011). Thus, the discussed short contacts Se···Cl$^-$, C–H···Cl$^-$ and Se···Se in the structure are attractive.

4. Database survey

A search in the Cambridge Structural Database (CSD, Version 5.43, update of Sep. 2022; Groom *et al.*, 2016) showed only 16 hits for 1,2,4-selenodiazolium salts, which differ not only in the type of nitrile fragment (Me: EWEPUU, Khrustalev *et al.*, 2021; Ph: NAQDES, Buslov *et al.*, 2021; BrC_6H_4: EWEQEF, Khrustalev *et al.*, 2021), but also in the anion (CF_3COO–: YEJXEU; $AuCl_4$–: YEJXUK; and ReO_4^-: YEJYAR, Artemjev *et al.*, 2022).

5. Synthesis and crystallization

General remarks. All manipulations were carried out in air. All the reagents used in this study were obtained from commercial sources (Aldrich, TCI-Europe, Strem, ABCR). Commercially available solvents were purified by conventional methods and distilled right before they were used. NMR spectra were recorded on a Bruker Advance Neo (^{1}H: 700 MHz); chemical shifts (δ) are given in ppm, coupling

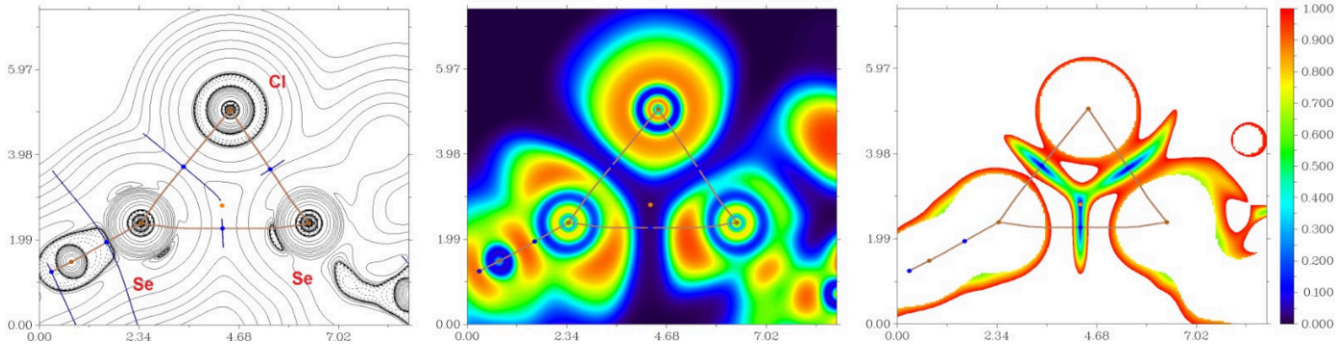

Figure 4
Contour line diagram of the Laplacian of the electron-density distribution $\tilde{N}^2 r(\mathbf{r})$, bond paths, and selected zero-flux surfaces (left panel), visualization of the electron localization function (ELF, center panel) and reduced density gradient (RDG, right panel) analyses for chalcogen bonding Se2···Se1^{i} [3.9426 (18) Å; symmetry code: (i) $x, \frac{3}{2} - y, \frac{1}{2} + z$], Se2···Cl1^{-ii} [3.229 (2) Å; symmetry code: (ii) $-x, \frac{1}{2} + y, \frac{1}{2} - z$] and Se1···Cl1^{-iii} [3.3805 (19) Å; symmetry code: (iii) $-x, 1 - y, -z$] in the crystal structure. Bond critical points (3, −1) are shown in blue, nuclear critical points (3, −3) in pale brown, ring critical points (3, +1) in orange, bond paths are shown as pale brown lines, length units in Å, and the color scale for the ELF and RDG maps is presented in a.u.

constants (J) in Hz. 2-Pyridylselenyl chloride was synthesized by our method (Artemjev *et al.*, 2022; Artemjev *et al.*, 2023).

A solution of phenylselenocyanate (0.16 mmol, 20 µL) in CH_2Cl_2 (1 mL) was added to a suspension of 2-pyridylselenyl chloride (0.13 mmol, 25.3 mg) in CH_2Cl_2 (2 mL) and the mixture was kept at room temperature for 6 h without stirring. The formed colorless precipitate was centrifuged, washed with CH_2Cl_2 (1 mL), Et_2O (3 × 1 mL) and dried under vacuum. Yield 34.5 mg (70%). ^{1}H NMR (700 MHz, D_2O) δ 9.53 (*d*, J = 6.8 Hz, 1H, H5), 8.82 (*d*, J = 8.6 Hz, 1H, H8), 8.42 (*t*, J = 7.9 Hz, 1H, H7), 8.05 (*t*, J = 7.0 Hz, 1H, H6), 7.82 (*d*, J = 7.6 Hz, 2H, H2′), 7.55 (*t*, J = 7.5 Hz, 1H, H4′), 7.49 (*t*, J = 7.7 Hz, 2H, H3′). ^{13}C NMR (176 MHz, D_2O) δ 168.1 (C3), 148.8 (C9), 139.9 (C5), 137.4 (C8), 135.7 (C2′), 130.5 (C4′), 130.3 (C3′), 126.0 (C7), 123.8 (C1′), 123.2 (C6). Crystals suitable for X-ray analysis were obtained directly from the reaction mixture.

The single-point calculations based on the experimental X-ray structure were carried out at the DFT level of theory using the dispersion-corrected hybrid functional ωB97XD (Chai *et al.*, 2008) with the *Gaussian-09* (Frisch *et al.*, 2010) program package. The 6-311++G** basis sets were used for all atoms. The topological analysis of the electron density distribution was performed using the *Multiwfn* program (version 3.7; Lu *et al.*, 2012). The Cartesian atomic coordinates for the model structure are presented in Table S1 of the supporting information.

Table 2
Experimental details.

Crystal data	
Chemical formula	$C_{12}H_9N_2Se_2^+\cdot Cl^-\cdot 0.352CH_2Cl_2$
M_r	404.50
Crystal system, space group	Monoclinic, $P2_1/c$
Temperature (K)	100
a, b, c (Å)	11.087 (3), 11.758 (5), 11.991 (3)
β (°)	115.337 (6)
V (Å^3)	1412.8 (8)
Z	4
Radiation type	Mo $K\alpha$
μ (mm^{-1})	5.54
Crystal size (mm)	0.20 × 0.10 × 0.08
Data collection	
Diffractometer	Bruker D8 Venture
Absorption correction	Multi-scan (*SADABS*; Krause *et al.*, 2015)
T_{min}, T_{max}	0.466, 0.746
No. of measured, independent and observed [$I > 2\sigma(I)$] reflections	7927, 3394, 2649
R_{int}	0.038
(sin $\theta/\lambda)_{max}$ (Å^{-1})	0.661
Refinement	
$R[F^2 > 2\sigma(F^2)]$, $wR(F^2)$, S	0.043, 0.088, 1.06
No. of reflections	3394
No. of parameters	182
No. of restraints	20
H-atom treatment	H-atom parameters constrained
$\Delta\rho_{max}$, $\Delta\rho_{min}$ (e Å^{-3})	1.50, −0.92

Computer programs: *APEX2* and *SAINT* (Bruker, 2019), *SHELXT2014/5* (Sheldrick, 2015*a*), *SHELXL2019/2* (Sheldrick, 2015*b*) and *OLEX2* (Dolomanov *et al.*, 2009).

6. Refinement

Crystal data, data collection and structure refinement details are summarized in Table 2. H atoms were included in calculated positions (C—H = 0.95–1.00 Å) and refined as riding with U_{iso}(H) = 1.2U_{eq}(C). The dichloromethane molecule is disordered around a center of symmetry and refined to a total occupancy of 70%. Residual electron density of 1.5 e Å^{-3} remained at the center of symmetry. Attempts to rationalize it did not produce a plausible model nor an improved refinement.

Funding information

This work was performed under the support of the Russian Science Foundation (award No. 22–73–10007).

References

Artemjev, A. A., Kubasov, A. S., Zaytsev, V. P., Borisov, A. V., Kritchenkov, A. S., Nenajdenko, V. G., Gomila, R. M., Frontera, A. & Tskhovrebov, A. G. (2023). *Cryst. Growth Des.* **23**, 2018–2023.

Artemjev, A. A., Novikov, A. P., Burkin, G. M., Sapronov, A. A., Kubasov, A. S., Nenajdenko, V. G., Khrustalev, V. N., Borisov, A. V., Kirichuk, A. A., Kritchenkov, A. S., Gomila, R. M., Frontera, A. & Tskhovrebov, A. G. (2022). *Int. J. Mol. Sci.* **23**, 63721–6372.

Bondi, A. (1966). *J. Phys. Chem.* **70**, 3006–3007.

Bruker (2019). *APEX2* and *SAINT*. Bruker AXS Inc., Madison, Wisconsin, USA.

Buslov, I. V., Novikov, A. S., Khrustalev, V. N., Grudova, M. V., Kubasov, A. S., Matsulevich, Z. V., Borisov, A. V., Lukiyanova, J. M., Grishina, M. M., Kirichuk, A. A., Serebryanskaya, T. V., Kritchenkov, A. S. & Tskhovrebov, A. G. (2021). *Symmetry*, **13**, 2350.

Chai, J.-D. & Head-Gordon, M. (2008). *Phys. Chem. Chem. Phys.* **10**, 6615–6620.

Contreras-García, J., Johnson, E. R., Keinan, S., Chaudret, R., Piquemal, J.-P., Beratan, D. N. & Yang, W. (2011). *J. Chem. Theory Comput.* **7**, 625–632.

Dolomanov, O. V., Bourhis, L. J., Gildea, R. J., Howard, J. A. K. & Puschmann, H. (2009). *J. Appl. Cryst.* **42**, 339–341.

Espinosa, E., Alkorta, I., Elguero, J. & Molins, E. (2002). *J. Chem. Phys.* **117**, 5529–5542.

Frisch, M. J., Trucks, G. W., Schlegel, H. B., Scuseria, G. E., Robb, M. A., Cheeseman, J. R., Scalmani, G., Barone, V., Mennucci, B., Petersson, G. A., Nakatsuji, H., Caricato, M., Li, X., Hratchian, H. P., Izmaylov, A. F., Bloino, J., Zheng, G., Sonnenberg, J. L., Had, M., Ehara, M., Toyota, K., Fukuda, R., Hasegawa, J., Ishida, M., Nakajima, T., Honda, Y., Kitao, O., Nakai, H., Vreven, T., Montgomery, J. A. Jr, Peralta, J. E., Ogliaro, F., Bearpark, M., Heyd, J. J., Brothers, E., Kudin, K. N., Staroverov, V. N., Kobayashi, R., Normand, J., Raghavachari, K., Rendell, A., Burant, J. C., Iyengar, S. S., Tomasi, J., Cossi, M., Rega, N., Millam, J. M., Klene, M., Knox, J. E., Cross, J. B., Bakken, V., Adamo, C., Jaramillo, J., Gomperts, R., Stratmann, R. E., Yazyev, O., Austin, A. J., Cammi, R., Pomelli, C., Ochterski, J. W., Martin, R. L., Morokuma, K., Zakrzewski, V. G., Voth, G. A., Salvador, P., Dannenberg, J. J., Dapprich, S., Daniels, A. D., Farkas, O., Foresman, J. B., Ortiz, J. V., Cioslowski, J. & Fox, D. J. (2010). *Gaussian 09, Revision B. 01*. Gaussian Inc. Wallingford, CT, USA.

Groom, C. R., Bruno, I. J., Lightfoot, M. P. & Ward, S. C. (2016). *Acta Cryst.* B**72**, 171–179.

Grudova, M. V., Kubasov, A. S., Khrustalev, V. N., Novikov, A. S., Kritchenkov, A. S., Nenajdenko, V. G., Borisov, A. V. & Tskhovrebov, A. G. (2022). *Molecules*, **27**, 10291–1029.

Gushchin, P. V., Kuznetsov, M. L., Haukka, M., Wang, M.-J., Gribanov, A. V. & Kukushkin, V. Y. (2009). *Inorg. Chem.* **48**, 2583–2592.
Johnson, E. R., Keinan, S., Mori-Sánchez, P., Contreras-García, J., Cohen, A. J. & Yang, W. (2010). *J. Am. Chem. Soc.* **132**, 6498–6506.
Khrustalev, V. N., Grishina, M. M., Matsulevich, Z. V., Lukiyanova, J. M., Borisova, G. N., Osmanov, V. K., Novikov, A. S., Kirichuk, A. A., Borisov, A. V., Solari, E. & Tskhovrebov, A. G. (2021). *Dalton Trans.* **50**, 10689–10691.
Krause, L., Herbst-Irmer, R., Sheldrick, G. M. & Stalke, D. (2015). *J. Appl. Cryst.* **48**, 3–10.
Kritchenkov, A. S., Bokach, N. A., Haukka, M. & Kukushkin, V. Y. (2011). *Dalton Trans.* **40**, 4175–4182.
Le Questel, J.-Y., Berthelot, M. & Laurence, C. (2000). *J. Phys. Org. Chem.* **13**, 347–358.
Lu, T. & Chen, F. (2012). *J. Comput. Chem.* **33**, 580–592.
Sapronov, A. A., Artemjev, A. A., Burkin, G. M., Khrustalev, V. N., Kubasov, A. S., Nenajdenko, V. G., Gomila, R. M., Frontera, A., Kritchenkov, A. S. & Tskhovrebov, A. G. (2022). *Int. J. Mol. Sci.* **23**, 14973.
Sapronov, A. A., Kubasov, A. S., Khrustalev, V. N., Artemjev, A. A., Burkin, G. M., Dukhnovsky, E. A., Chizhov, A. O., Kritchenkov, A. S., Gomila, R. M., Frontera, A. & Tskhovrebov, A. G. (2023). *Symmetry* **15**, 212.
Sheldrick, G. M. (2015*a*). *Acta Cryst.* A**71**, 3–8.
Sheldrick, G. M. (2015*b*). *Acta Cryst.* C**71**, 3–8.

supporting information

Acta Cryst. (2024). E**80**, 1024-1028 [https://doi.org/10.1107/S2056989024008831]

Coupling between 2-pyridylselenyl chloride and phenylselenocyanate: synthesis, crystal structure and non-covalent interactions

Ayalew W. Temesgen, Alexander G. Tskhovrebov, Alexey A. Artemjev, Alexey S. Kubasov, Alexander S. Novikov, Alexander V. Borisov, Anatoly A. Kirichuk, Andreii S. Kritchenkov and Tuan Anh Le

Computing details

3-(Phenylselanyl)[1,2,4]selenadiazolo[4,5-*a*]pyridin-4-ylium chloride dichloromethane

Crystal data

$C_{12}H_9N_2Se_2^+ \cdot Cl^- \cdot 0.352CH_2Cl_2$
$M_r = 404.50$
Monoclinic, $P2_1/c$
$a = 11.087$ (3) Å
$b = 11.758$ (5) Å
$c = 11.991$ (3) Å
$\beta = 115.337$ (6)°
$V = 1412.8$ (8) Å^3
$Z = 4$
$F(000) = 779$
$D_x = 1.902$ Mg m^{-3}
Mo $K\alpha$ radiation, $\lambda = 0.71073$ Å
Cell parameters from 3887 reflections
$\theta = 2.6$–$28.0°$
$\mu = 5.54$ mm^{-1}
$T = 100$ K
Block, colourless
0.20 × 0.10 × 0.08 mm

Data collection

Bruker D8 Venture diffractometer
φ and ω scans
Absorption correction: multi-scan (SADABS; Krause *et al.*, 2015)
$T_{min} = 0.466$, $T_{max} = 0.746$
7927 measured reflections
3394 independent reflections
2649 reflections with $I > 2\sigma(I)$
$R_{int} = 0.038$
$\theta_{max} = 28.0°$, $\theta_{min} = 2.0°$
$h = -12 \rightarrow 14$
$k = -12 \rightarrow 15$
$l = -15 \rightarrow 15$

Refinement

Refinement on F^2
Least-squares matrix: full
$R[F^2 > 2\sigma(F^2)] = 0.043$
$wR(F^2) = 0.088$
$S = 1.06$
3394 reflections
182 parameters
20 restraints
Primary atom site location: dual
Secondary atom site location: difference Fourier map
Hydrogen site location: mixed
H-atom parameters constrained
$w = 1/[\sigma^2(F_o^2) + (0.0153P)^2 + 6.8557P]$ where $P = (F_o^2 + 2F_c^2)/3$
$(\Delta/\sigma)_{max} < 0.001$
$\Delta\rho_{max} = 1.50$ e Å^{-3}
$\Delta\rho_{min} = -0.91$ e Å^{-3}

Special details

Geometry. All esds (except the esd in the dihedral angle between two l.s. planes) are estimated using the full covariance matrix. The cell esds are taken into account individually in the estimation of esds in distances, angles and torsion angles; correlations between esds in cell parameters are only used when they are defined by crystal symmetry. An approximate (isotropic) treatment of cell esds is used for estimating esds involving l.s. planes.

Fractional atomic coordinates and isotropic or equivalent isotropic displacement parameters (Å²)

	x	*y*	*z*	U_{iso}*/U_{eq}	Occ. (<1)
Se1	0.10761 (5)	0.56698 (4)	0.17359 (4)	0.01592 (12)	
Se2	0.24558 (5)	0.87121 (4)	0.42629 (4)	0.01426 (12)	
N1	0.1762 (4)	0.6289 (3)	0.4071 (4)	0.0132 (8)	
N2	0.1584 (4)	0.7155 (3)	0.2272 (4)	0.0162 (8)	
C1	0.1373 (4)	0.5329 (4)	0.3362 (4)	0.0121 (9)	
C2	0.1221 (5)	0.4305 (4)	0.3880 (4)	0.0150 (9)	
H2	0.095583	0.363323	0.339559	0.018*	
C3	0.1465 (5)	0.4290 (4)	0.5109 (5)	0.0188 (10)	
H3	0.138254	0.359887	0.548151	0.023*	
C4	0.1833 (5)	0.5294 (4)	0.5812 (4)	0.0183 (10)	
H4	0.197564	0.528274	0.665125	0.022*	
C5	0.1988 (5)	0.6283 (4)	0.5295 (4)	0.0143 (9)	
H5	0.224770	0.695960	0.577185	0.017*	
C6	0.1880 (5)	0.7279 (4)	0.3425 (4)	0.0134 (9)	
C7	0.4343 (5)	0.8524 (4)	0.4672 (5)	0.0162 (10)	
C8	0.5220 (5)	0.8288 (4)	0.5882 (5)	0.0259 (12)	
H8	0.488948	0.818120	0.648615	0.031*	
C9	0.6579 (6)	0.8207 (5)	0.6214 (5)	0.0319 (13)	
H9	0.717735	0.804495	0.704425	0.038*	
C10	0.7062 (5)	0.8362 (4)	0.5339 (6)	0.0281 (13)	
H10	0.799414	0.831392	0.556943	0.034*	
C11	0.6195 (5)	0.8587 (5)	0.4130 (5)	0.0276 (12)	
H11	0.653058	0.868078	0.352710	0.033*	
C12	0.4828 (5)	0.8677 (5)	0.3788 (5)	0.0238 (11)	
H12	0.423253	0.884189	0.295774	0.029*	
Cl1	0.05719 (12)	0.32474 (9)	0.11352 (11)	0.0163 (2)	
Cl2	0.5173 (17)	0.4244 (7)	0.6117 (12)	0.055 (2)	0.352 (3)
Cl3	0.4753 (18)	0.5382 (9)	0.3886 (13)	0.077 (3)	0.352 (3)
C13	0.5222 (19)	0.5578 (8)	0.5473 (13)	0.058 (4)	0.352 (3)
H13A	0.613356	0.590037	0.587480	0.069*	0.352 (3)
H13B	0.459970	0.611151	0.559777	0.069*	0.352 (3)

Atomic displacement parameters (Å²)

	U^{11}	U^{22}	U^{33}	U^{12}	U^{13}	U^{23}
Se1	0.0243 (3)	0.0133 (2)	0.0105 (2)	−0.0043 (2)	0.0078 (2)	−0.00122 (19)
Se2	0.0161 (2)	0.0113 (2)	0.0162 (2)	−0.00220 (19)	0.0076 (2)	−0.00216 (19)
N1	0.016 (2)	0.0113 (17)	0.014 (2)	−0.0002 (16)	0.0076 (17)	−0.0001 (16)
N2	0.023 (2)	0.0122 (18)	0.013 (2)	−0.0050 (17)	0.0073 (18)	0.0000 (16)

C1	0.013 (2)	0.012 (2)	0.012 (2)	−0.0013 (18)	0.0052 (19)	0.0001 (17)
C2	0.017 (2)	0.012 (2)	0.016 (2)	−0.0004 (19)	0.008 (2)	−0.0013 (19)
C3	0.018 (2)	0.018 (2)	0.021 (3)	0.000 (2)	0.009 (2)	0.005 (2)
C4	0.024 (3)	0.021 (2)	0.010 (2)	−0.002 (2)	0.008 (2)	−0.0019 (19)
C5	0.021 (2)	0.013 (2)	0.009 (2)	0.005 (2)	0.0062 (19)	−0.0008 (18)
C6	0.014 (2)	0.013 (2)	0.015 (2)	0.0005 (18)	0.007 (2)	0.0008 (18)
C7	0.015 (2)	0.009 (2)	0.022 (3)	−0.0017 (18)	0.005 (2)	−0.0016 (19)
C8	0.024 (3)	0.027 (3)	0.023 (3)	−0.003 (2)	0.008 (2)	−0.002 (2)
C9	0.019 (3)	0.032 (3)	0.029 (3)	0.001 (2)	−0.005 (2)	0.001 (3)
C10	0.014 (3)	0.016 (2)	0.049 (4)	0.000 (2)	0.008 (3)	−0.007 (2)
C11	0.025 (3)	0.028 (3)	0.034 (3)	−0.001 (2)	0.016 (3)	−0.003 (2)
C12	0.017 (3)	0.029 (3)	0.023 (3)	0.000 (2)	0.006 (2)	−0.002 (2)
Cl1	0.0179 (6)	0.0140 (5)	0.0172 (6)	−0.0004 (5)	0.0078 (5)	−0.0028 (4)
Cl2	0.043 (3)	0.040 (5)	0.088 (4)	−0.012 (4)	0.033 (3)	−0.019 (4)
Cl3	0.047 (4)	0.070 (7)	0.113 (5)	−0.004 (6)	0.035 (4)	−0.004 (6)
C13	0.036 (6)	0.049 (7)	0.096 (7)	−0.013 (7)	0.036 (6)	0.005 (7)

Geometric parameters (Å, º)

Se1—N2	1.863 (4)	C7—C8	1.385 (7)
Se1—C1	1.877 (4)	C7—C12	1.390 (7)
Se2—C6	1.926 (5)	C8—C9	1.388 (7)
Se2—C7	1.946 (5)	C8—H8	0.9500
N1—C1	1.367 (6)	C9—C10	1.379 (8)
N1—C5	1.380 (6)	C9—H9	0.9500
N1—C6	1.435 (6)	C10—C11	1.380 (8)
N2—C6	1.285 (6)	C10—H10	0.9500
C1—C2	1.396 (6)	C11—C12	1.395 (7)
C2—C3	1.380 (6)	C11—H11	0.9500
C2—H2	0.9500	C12—H12	0.9500
C3—C4	1.405 (7)	Cl2—C13	1.7596 (12)
C3—H3	0.9500	Cl3—C13	1.7597 (11)
C4—C5	1.362 (6)	C13—H13A	0.9900
C4—H4	0.9500	C13—H13B	0.9900
C5—H5	0.9500		
N2—Se1—C1	87.06 (18)	C8—C7—C12	119.8 (5)
C6—Se2—C7	96.45 (18)	C8—C7—Se2	118.9 (4)
C1—N1—C5	121.5 (4)	C12—C7—Se2	121.2 (4)
C1—N1—C6	114.4 (4)	C7—C8—C9	120.2 (5)
C5—N1—C6	124.2 (4)	C7—C8—H8	119.9
C6—N2—Se1	112.2 (3)	C9—C8—H8	119.9
N1—C1—C2	120.1 (4)	C10—C9—C8	120.0 (5)
N1—C1—Se1	109.7 (3)	C10—C9—H9	120.0
C2—C1—Se1	130.2 (3)	C8—C9—H9	120.0
C3—C2—C1	118.7 (4)	C9—C10—C11	120.1 (5)
C3—C2—H2	120.6	C9—C10—H10	119.9
C1—C2—H2	120.6	C11—C10—H10	119.9

C2—C3—C4	120.2 (4)	C10—C11—C12	120.3 (5)
C2—C3—H3	119.9	C10—C11—H11	119.9
C4—C3—H3	119.9	C12—C11—H11	119.9
C5—C4—C3	120.3 (4)	C7—C12—C11	119.5 (5)
C5—C4—H4	119.8	C7—C12—H12	120.2
C3—C4—H4	119.8	C11—C12—H12	120.2
C4—C5—N1	119.2 (4)	Cl2—C13—Cl3	107.9 (5)
C4—C5—H5	120.4	Cl2—C13—H13A	110.1
N1—C5—H5	120.4	Cl3—C13—H13A	110.1
N2—C6—N1	116.6 (4)	Cl2—C13—H13B	110.1
N2—C6—Se2	122.4 (3)	Cl3—C13—H13B	110.1
N1—C6—Se2	121.0 (3)	H13A—C13—H13B	108.4
C1—Se1—N2—C6	−0.4 (4)	Se1—N2—C6—N1	−0.5 (5)
C5—N1—C1—C2	−1.3 (7)	Se1—N2—C6—Se2	179.5 (2)
C6—N1—C1—C2	179.9 (4)	C1—N1—C6—N2	1.5 (6)
C5—N1—C1—Se1	177.1 (3)	C5—N1—C6—N2	−177.3 (4)
C6—N1—C1—Se1	−1.6 (5)	C1—N1—C6—Se2	−178.6 (3)
N2—Se1—C1—N1	1.1 (3)	C5—N1—C6—Se2	2.7 (6)
N2—Se1—C1—C2	179.4 (5)	C12—C7—C8—C9	0.1 (8)
N1—C1—C2—C3	0.4 (7)	Se2—C7—C8—C9	−176.7 (4)
Se1—C1—C2—C3	−177.7 (4)	C7—C8—C9—C10	0.0 (8)
C1—C2—C3—C4	1.1 (7)	C8—C9—C10—C11	−0.6 (8)
C2—C3—C4—C5	−1.7 (7)	C9—C10—C11—C12	1.0 (8)
C3—C4—C5—N1	0.8 (7)	C8—C7—C12—C11	0.3 (8)
C1—N1—C5—C4	0.7 (7)	Se2—C7—C12—C11	177.0 (4)
C6—N1—C5—C4	179.4 (4)	C10—C11—C12—C7	−0.8 (8)

Hydrogen-bond geometry (Å, º)

D—H···*A*	*D*—H	H···*A*	*D*···*A*	*D*—H···*A*
C2—H2···Cl1	0.95	2.60	3.297 (5)	131
C3—H3···Cl1^{i}	0.95	2.60	3.526 (5)	167
C5—H5···Se2	0.95	2.82	3.242 (5)	108
C5—H5···N2^{ii}	0.95	2.45	3.179 (6)	134

Symmetry codes: (i) *x*, −*y*+1/2, *z*+1/2; (ii) *x*, −*y*+3/2, *z*+1/2.